GEOCHEMISTRY

Late delivery of exotic chromium to the crust of Mars by water-rich carbonaceous asteroids

Ke Zhu[1]†, Martin Schiller[2], Lu Pan[2], Nikitha Susan Saji[2], Kirsten K. Larsen[2], Elsa Amsellem[2], Courtney Rundhaug[2], Paolo Sossi[3], Ingo Leya[4], Frederic Moynier[1], Martin Bizzarro[1,2]*

The terrestrial planets endured a phase of bombardment following their accretion, but the nature of this late accreted material is debated, preventing a full understanding of the origin of inner solar system volatiles. We report the discovery of nucleosynthetic chromium isotope variability (μ^{54}Cr) in Martian meteorites that represent mantle-derived magmas intruded in the Martian crust. The μ^{54}Cr variability, ranging from −33.1 ± 5.4 to +6.8 ± 1.5 parts per million, correlates with magma chemistry such that samples having assimilated crustal material define a positive μ^{54}Cr endmember. This compositional endmember represents the primordial crust modified by impacting outer solar system bodies of carbonaceous composition. Late delivery of this volatile-rich material to Mars provided an exotic water inventory corresponding to a global water layer >300 meters deep, in addition to the primordial water reservoir from mantle outgassing. This carbonaceous material may also have delivered a source of biologically relevant molecules to early Mars.

INTRODUCTION

The terrestrial planets endured an early period of intense bombardment that postdates their main accretion phase from asteroids leftover from the main planetary growth stage (*1*). These bombardment episodes are modeled to result in compositional modification of planetary crusts by assimilation of impacting bolides, which can potentially deliver exotic material to the planets' surfaces (*2*). However, it remains debated whether the late accreted material was derived from the inner or outer solar system and, hence, whether it was rich in volatile elements (*3*–*6*). Elucidating the nature and composition of the late accreted material is critical, as it may provide a source of volatiles, including water, to terrestrial planets.

Mars is a planetary embryo that accreted and differentiated within the ~5-Ma lifetime of the solar protoplanetary disk (*7*, *8*), resulting in the isotopic homogenization of the planet's precursor material via a vigorously convecting global magma ocean phase (*9*). Planetary differentiation processes, including the dynamics of the crust-mantle system, can be inferred from the study of Martian meteorites. These include shergottites, nakhlites, and chassignites, representing mantle-derived, near-surface extrusive lavas or hypabyssal rocks intruded within the Martian crust (*10*). These meteorites record extreme isotopic and chemical diversity, which provides evidence for the existence of geochemically enriched and depleted reservoirs established early in the planet's history (*11*). Moreover, the existence of mass-independent sulfur isotope anomalies in several Martian meteorites (*12*), a fingerprint of atmospheric photochemical processing, indicate that assimilation of crustal materials into Martian magmas occurred throughout the planet's history. Thus, Martian meteorites offer clues with respect to the composition of the primordial crust of Mars, including the existence of exotic material at the planet's surface.

It is well established from the meteorite record and remote sensing that Mars experienced substantial reworking of its primordial crust by intense bombardment episodes early in its evolution (*13*–*15*). These energetic impacts are predicted to result in significant remelting of the primordial crust (*16*) and, in turn, compositional modification by assimilation of impacting bolides. Given the large-scale nucleosynthetic heterogeneity that exists among solar system rocky bodies (*17*), compositional modification of the crust by admixing of impacting material may result in a shift in the nucleosynthetic makeup of the crust relative to that of the primitive mantle. As Mars lacks plate tectonics, this signature will be preserved in the Martian crust over the entire geologic history of the planet. Thus, progressive assimilation of crustal material by mantle-derived magmas will lead to a trackable change in the nucleosynthetic makeup of the contaminated lithologies.

RESULTS

Nucleosynthetic heterogeneity recorded by Martian meteorites

Chromium isotopes provide insights into the nucleosynthetic history and the formation time scales of planetary reservoirs. The solar system's asteroids and planets preserve initial heterogeneity in their mass-independent $^{54}Cr/^{52}Cr$ ratios (μ^{54}Cr), corresponding to 250 parts per million (ppm) (*18*). Moreover, ^{53}Cr is the decay product of the short-lived ^{53}Mn nuclide (half-life of 3.7 Ma) such that Mn/Cr fractionation events during the lifetime of ^{53}Mn will result in mass-independent $^{53}Cr/^{52}Cr$ variability (μ^{53}Cr). To search for the isotopic signal of exotic Cr potentially present in the Martian crust, we conducted ultrahigh precision Cr isotope measurements of Martian meteorites. These measurements further allow us to determine the tempo of primordial crust extraction using the short-lived ^{53}Mn-^{53}Cr chronometer. Our samples include shergottites, nakhlites, one chassignite, the ALH84001 orthopyroxenite, and the NWA 7533 breccia, which represents a fragment of the ancient regolith of Mars. The external reproducibility of our μ^{54}Cr and μ^{53}Cr measurements corresponds to 7 and 4 ppm, respectively, representing a significant improvement over published data (*19*). These measurements are complemented by mass-dependent Cr isotope compositions (δ^{53}Cr)

[1]Université de Paris, Institut de Physique du Globe de Paris, Paris, France. [2]Centre for Star and Planet Formation, Globe Institute, University of Copenhagen, Copenhagen, Denmark. [3]Institute of Geochemistry and Petrology, ETH Zürich, Zürich, Switzerland. [4]Physics Institute, University of Bern, Bern, Switzerland.
*Corresponding author. Email: bizzarro@sund.ku.dk
†Present address: Bristol Isotope Group, School of Earth Sciences, University of Bristol, United Kingdom.

using double-spike techniques and major and trace element data obtained on the same aliquots used for Cr isotope determinations. Moreover, we acquired Sm isotope data for a subset of the samples to evaluate potential cosmogenic effects on the measured Cr isotopes.

We show in Fig. 1 that correlated variability exists in the $\mu^{54}Cr$ and $\mu^{53}Cr$ compositions of Martian meteorites. The range of $\mu^{54}Cr$ and $\mu^{53}Cr$ variability corresponds to 40.2 ± 5.3 and 14.5 ± 4.0 ppm, respectively, which is at least a factor of 3 greater than the analytical resolution of our technique. As the $\mu^{54}Cr$ and $\mu^{53}Cr$ variability is relatively small, it could reflect inappropriate correction for natural mass-dependent fractionation affecting the samples. However, recalculating the $\mu^{54}Cr$ and $\mu^{53}Cr$ values assuming different mass fractionation laws to account for the natural mass fractionation experienced by the samples results in a comparable range of $\mu^{54}Cr$ and $\mu^{53}Cr$ compositions (fig. S1). Moreover, we note that ALHA 77005 and MIL 090032 that define a $\mu^{54}Cr$ offset of 37.8 ± 6.1 ppm

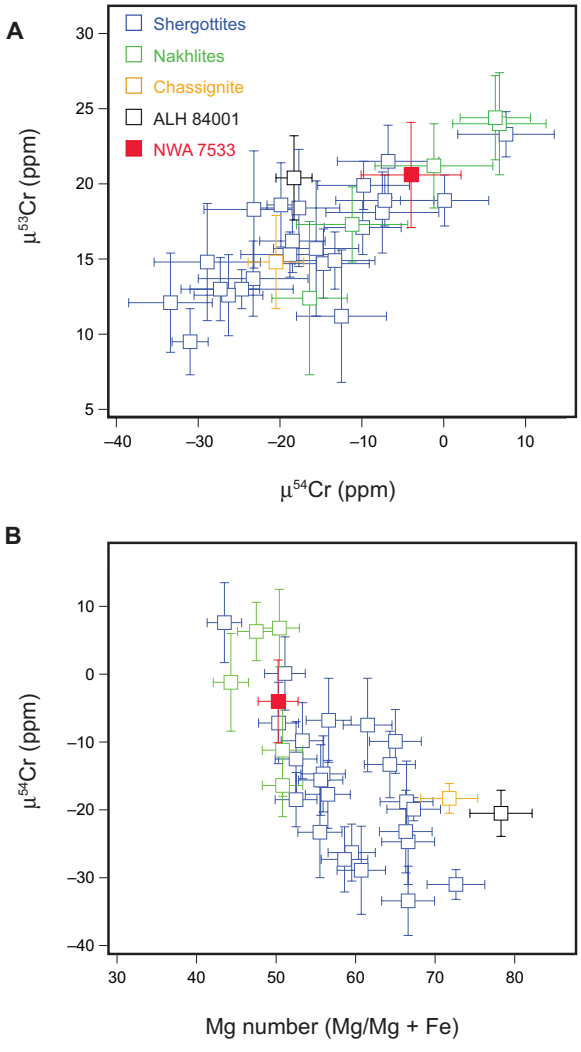

Fig. 1. Chromium mass-independent isotope compositions ($\mu^{53}Cr$ and $\mu^{54}Cr$) and Mg number. Shown in (**A**) is the $\mu^{54}Cr$ versus the $\mu^{53}Cr$ for samples analyzed in this study. The correlation defines a slope and intercept of 2.31 ± 0.60 and −53.3 ± 10.4 (95% confidence interval), respectively, with an r^2 of 0.81. In (**B**), we show that the $\mu^{54}Cr$ values are correlated to the Mg number (Mg/Fe + Mg), an index of magmatic differentiation. Uncertainties reflect internal errors (2SE).

record $\delta^{53}Cr$ values of −0.10 ± 0.02 and −0.18 ± 0.02, respectively. The maximum offset that can be attributed to inappropriate correction for natural mass-dependent fractionation affecting these two samples (i.e., equilibrium as opposed to kinetic mass fractionation law) is 8 ppm and, thus, cannot account for the observed variability. Likewise, 10 of our samples do not show evidence for stable isotope fractionation ($\delta^{53}Cr$ of −0.11 ± 0.02) relative to the composition of the bulk silicate Earth such that any $\mu^{54}Cr$ and $\mu^{53}Cr$ variability recorded by these sample cannot be ascribed to inappropriate correction for natural mass-dependent fractionation. However, these 10 samples define a range of $\mu^{54}Cr$ and $\mu^{53}Cr$ composition that span nearly the entire spectrum defined by all our samples (fig. S1). These observations establish that the observed variability cannot result from inappropriate correction for natural mass-dependent fractionation. Alternatively, the correlated $\mu^{54}Cr$-$\mu^{53}Cr$ variability could reflect neutron-capture effects. In this model, the sample with the lowest $\mu^{54}Cr$ and $\mu^{53}Cr$ values (ALHA 77005) represents the primary planetary composition, which requires a spallogenic production of ~15 and ~40 ppm for the $\mu^{53}Cr$ and $\mu^{54}Cr$ values, respectively. However, the $^{150}Sm/^{152}Sm$ ($\mu^{150}Sm$) ratios measured for a subset of our samples with variable $\mu^{54}Cr$ values return a homogenous $\mu^{150}Sm$ composition of 26 ± 4 ppm relative to Earth (fig. S2), which we interpret as a nucleosynthetic r–process excess in Mars similar to that observed for Nd isotopes (*20*, *21*). Moreover, to assess the potential effects on Cr isotopes from spallation of high-energy particles on the target element Fe during the meteoroid phase, we calculated the production rate of spallogenic Cr for various Fe/Cr ratios and exposure ages that are typical for our samples. We calculated the productions rates, assuming that the meteorites that we studied had preatmospheric radii ranging from 8 to 50 cm (see Supplementary Text). Using the highest Fe/Cr ratios in our samples and upper limits of 5 and 15 Ma for the exposure ages of shergottites and nakhlites, respectively, we show in fig. S3 that the effects on the $\mu^{54}Cr$ and $\mu^{53}Cr$ values are at most 1 ppm in all models and, thus, are clearly negligible. We conclude that the $\mu^{54}Cr$ and $\mu^{53}Cr$ variability expressed in Martian meteorites reflects their primary compositions.

The samples defining the high $\mu^{54}Cr$-$\mu^{53}Cr$ endmember in Fig. 1 are two nakhlites (MIL 03346 and MIL 090032) and one evolved shergottite (NWA 7320) characterized by low Mg# (<50) and superchondritic Mn/Cr ratios. In contrast, the low compositional endmember is defined by a primitive shergottite (ALHA 77005) typified by a high Mg# (>70) and subchondritic Mn/Cr ratio (table S1), suggesting that the $\mu^{54}Cr$-$\mu^{53}Cr$ variability may be a by-product of magmatic differentiation processes. We show in fig. S4 the $\mu^{54}Cr$-$\mu^{53}Cr$ and $\mu^{54}Cr$-Mg# correlation diagrams for shergottites grouped according to their level of light rare earth element enrichment, namely, depleted, intermediate, and enriched. A compositional range exists for the three types, with the intermediate and enriched shergottites extending to the high $\mu^{54}Cr$-$\mu^{53}Cr$ endmember. Fractional crystallization is known to have played a role in generating some of the geochemical diversity observed in Martian meteorites (*22*). In terrestrial systems, pyroxene and chromite fractionation during the magmatic evolution of mafic magmas results in progressive enrichment of the evolving magmas in the light Cr isotopes (*23*), a process that depletes the residual magma in Cr, as chromite is a major Cr reservoir. The $\mu^{54}Cr$ values correlate in a systematic way with typical indices of magmatic differentiation such as the Mg# (Fig. 1B); the $\delta^{53}Cr$ values; and the Fe/Cr, Al/Cr, and Mn/Cr ratios (Fig. 2). Using the Fe/Cr ratio as a proxy for the Cr concentration (fig. S5), Fig. 2C demonstrates that

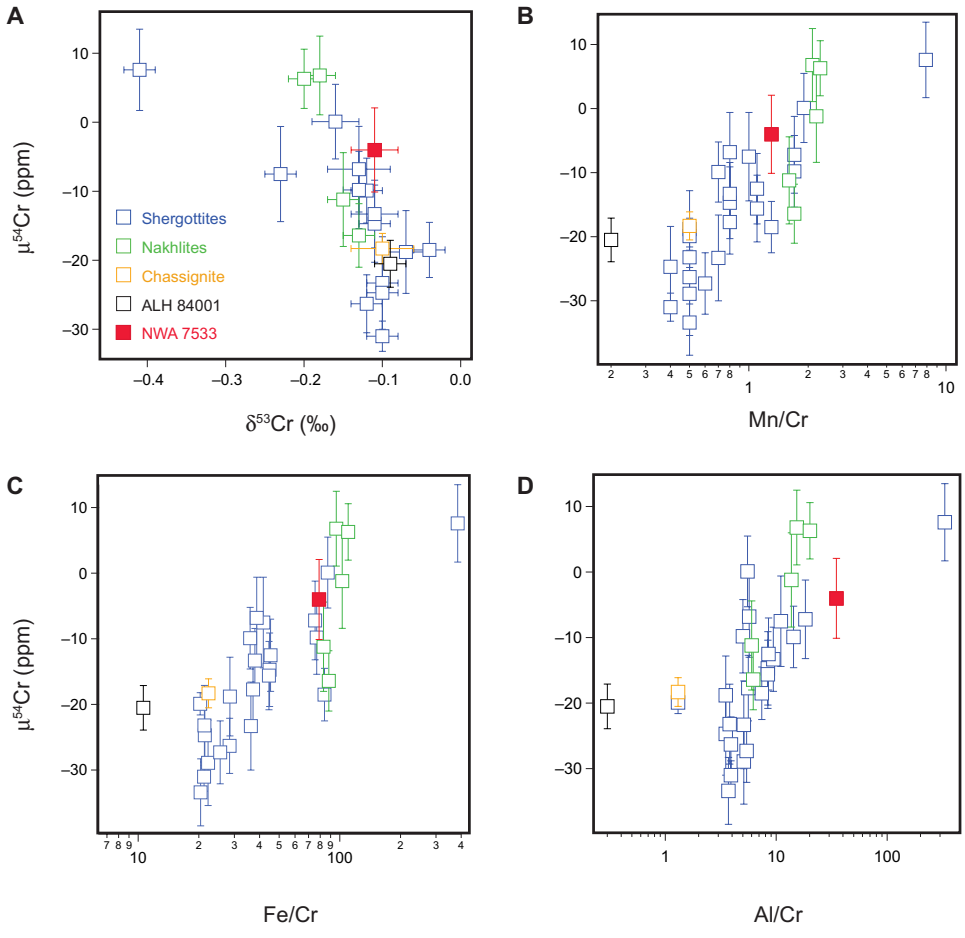

Fig. 2. Relationship between chromium mass-independent ($\mu^{54}Cr$) and mass-dependent ($\delta^{53}Cr$) isotope composition and indices of magmatic differentiation (Mn/Cr, Fe/Cr, and Al/Cr). Uncertainties represent internal precisions (2SE) for $\mu^{54}Cr$ values whereas we use a 10% uncertainty (smaller than symbols) for the elemental ratios.

samples defining positive $\mu^{54}Cr$ compositions have the lowest inferred Cr concentrations, establishing that the preservation of an exotic Cr isotope signal is a function of the initial Cr concentration of the magmas. Thus, the isotope fingerprint of assimilation of exotic Cr is most noticeable in Cr-poor evolved shergottites and nakhlites, whereas the Cr-rich parental magmas of less evolved shergottites and chassignites are impervious to this assimilation. A fractional crystallization model (see Supplementary Text) indicates that, under oxygen fugacity conditions recorded by Martian meteorites, significant levels of Cr depletion occur during magmatic evolution such that modest amounts of crustal assimilation (<5%) are required to generate the observed $\mu^{54}Cr$ variability. Critically, the nakhlites (MIL03346 and MIL 090032) that define the crustal endmember with a positive $\mu^{54}Cr$ composition record mass-independent sulfur isotope effects indicative of interaction with a crustal reservoir (*12*, *24*), in agreement with our interpretation. We emphasize that the observed $\mu^{54}Cr$ heterogeneity is not predicted to exist for nucleosynthetic tracers that behave incompatibly during magmatic differentiation such as ^{50}Ti and ^{48}Ca.

Admixing of exotic Cr in the Martian crust by impacts

The Cr isotope data require that mantle-derived magmas on Mars interacted with a reservoir enriched in ^{54}Cr before or during their eruption at the planet's surface. An efficient means of delivering exotic Cr is from impacting bodies, which can result in admixing of bolide material to planet's crust and mantle. The $\mu^{54}Cr$ compositions of the most evolved lithologies, interpreted to have been readily affected by assimilation of exotic Cr, provides a means of identifying its source. The three samples with the highest $\mu^{54}Cr$ values define a mean of 6.8 ± 1.5 ppm, which requires that the source of exotic Cr comes from asteroids with $\mu^{54}Cr$-rich compositions. Thus, the only plausible source of exotic Cr are the parent bodies of carbonaceous chondrites, characterized by $\mu^{54}Cr$ values ranging from ~50 to ~160 ppm (*25*), thereby ruling out noncarbonaceous material as a significant source of late accreted asteroids. The observation that the evolved NWA 7320 shergottite, characterized by a highly fractionated $\delta^{53}Cr$ value, records the same $\mu^{54}Cr$ value, as the two evolved nakhlites (Fig. 2A) has two important implications. First, it establishes that the exotic Cr was assimilated by the host magma of NWA 7320 before its subsequent differentiation, requiring that assimilation of exotic Cr occurred in a magma chamber located within a crustal reservoir. Second, it implies that the $\mu^{54}Cr$ value of 6.8 ± 1.5 ppm recorded by three samples with variable $\delta^{53}Cr$ values must reflect that of the assimilated Martian crust. Thus, our results indicate the bulk Cr isotope composition of the Martian crust has been modified by impacting bodies of carbonaceous compositions from the outer solar system.

Recent work on the Martian meteorite breccia NWA 7533 (and its pairs) suggests that significant reworking and remelting of the primordial crust occurred during the first ~100 Ma of the planet's history by bombardment (*13*, *14*, *26*). This epoch also comprises the estimated formation time of the source reservoir of shergottites (*27*), which has been linked to the formation of the Martian crustal dichotomy by a giant impact after extraction of the primordial crust (*28*). This bombardment episode has been attributed to the early migration of the gas giant planets that caused a flux of asteroidal and cometary bodies to the terrestrial planet–forming region (*3*). Recent dynamical models that explore the origin of the source material impacting the terrestrial planets, including outer asteroid belt bodies and comets, concluded that for Mars, the impacting material will be dominated by cometary bodies (*29*). This conclusion is consistent with the carbonaceous nature of the exotic Cr component identified in the Martian crust, which requires an outer solar system origin.

The Renazzo-type carbonaceous (CR) chondrites are inferred to have formed in an outer solar system reservoir that is distinct from most carbonaceous chondrites, possibly initially located beyond the gas giants where cometary objects accreted (*30*, *31*). Thus, CR chondrites provide a proxy for the composition of the material accreted beyond Neptune and delivered to the terrestrial planet–forming region in the aftermath of the migration of the gas giants (see Supplementary Text). Using the average Cr concentration and μ^{54}Cr value of CR chondrites (*25*), an initial Cr concentration of 2500 ppm and a μ^{54}Cr value of −33 ppm for the primordial crust, our data require that 24% of chondritic material has been admixed to the Martian crust to reproduce the measured value of μ^{54}Cr 6.8 ± 1.5 for the crustal endmember (Material and Methods). To evaluate this conclusion, we determined the accumulated mass of impactor material delivered to Mars before 4.1 Ga based on two approaches, which provide a lower limit to the pre-Noachian impactor flux (Material and Methods). First, we consider the observational evidence for early impactors on Mars from buried impact basins, including only the oldest large impact basins (*32*) with a Crater Ray Age greater than 2. Second, we include the dichotomy-forming impact (*28*) as a possible major event that delivered chondritic materials to the Martian surface. We show in Fig. 3 that the mass required to match our observations is achieved in two scenarios. A model that includes the oldest large impact basins results in a mass of ~4.5×10^{20} kg, which, if mixed in the first ~4 km of the Martian crust, provides the required composition. Alternatively, including the dichotomy-forming impact increases the total mass of bolide material to ~6×10^{21} kg. If mixed with the entire thickness of the Martian crust, then this amount of material can account for the observed ^{54}Cr composition of the crustal endmember identified here. We note that the minimum estimate of ~4.5×10^{20} kg determined here for the cometary flux to Mars compares favorably with that of ~2.6 to 3.0×10^{20} kg inferred from recent numerical simulation (*29*). Although our impact model assumes homogeneous distribution of bolide material in the crust, vertical and lateral heterogeneity is expected to be preserved. For example, the inferred μ^{54}Cr excess of 6.8 ± 1.5 ppm for the crust recorded by nakhlites and shergottites is different from that of −4.0 ± 6.1 ppm preserved in the NWA 7533 regolith breccia. However, the observation that ^{54}Cr-rich compositions distinct from the primordial mantle value (~−30 ppm) are recorded by samples with variable ages and geographical origins and derived from different mantle source regions (nakhlites, enriched and depleted shergottites, and NWA 7533) suggests that the ^{54}Cr enrichment is a generic feature of the Martian crust.

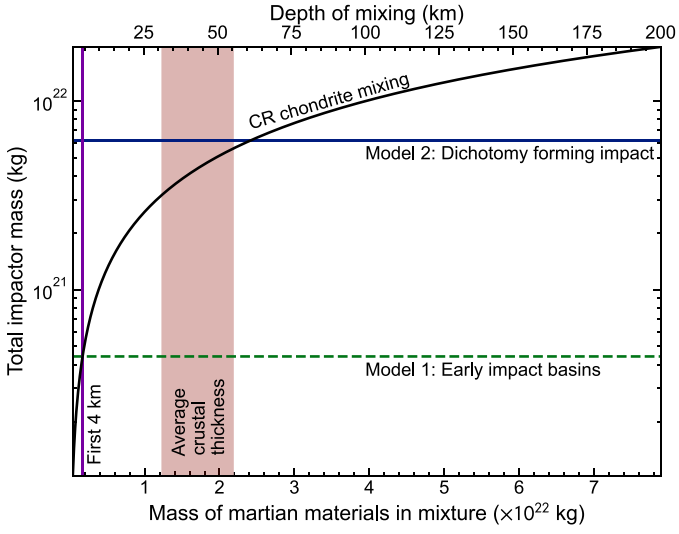

Fig. 3. Mixing model between an incoming flux of outer solar system chondritic impactor and the crust of Mars. The model describes a scenario where the observed Cr isotopic composition of the crust (μ^{54}Cr of 6.8 ± 1.5 ppm) can be explained by mixing the anomalous composition of incoming impactor flux before 4.1 Ga modeled to be CR chondrite-like (μ^{54}Cr of 128 ± 4 ppm) and requires a fraction of impactor material of 24% to satisfy the observed composition (see Materials and Methods). Two models are considered, namely, the old, buried basins (model 1) (*32*) and the dichotomy-forming impact (model 2) (*28*). Pink vertical bar represents the range of average crustal thickness from the results of seismic data from the InSight mission (*35*). Both cases can account for the observed μ^{54}Cr of the crustal endmember if the impactor mass is admixed to the first 5 km of the crust (model 1) or the entire thickness of the crust (model 2).

DISCUSSION

Formation time scale of Mars' main geochemical reservoirs

The evolved shergottite and the two nakhlites that define the crustal endmember based on the μ^{54}Cr data record a mean μ^{53}Cr value of 24 ± 2 ppm. However, using the mixing relationship derived from the μ^{54}Cr data, it is not possible to impart measurable variability in μ^{53}Cr that correlates with μ^{54}Cr. This is because of the limited range of μ^{53}Cr compositions that exists between the crust and mantle of planetary bodies relative to that of carbonaceous chondrites (*25*), which makes planetary crust and mantle impervious to ^{53}Cr contamination by chondritic bodies. Thus, the variability of 14.1 ± 2.3 ppm observed between the mantle and crustal end members of Mars can only reflect Mn/Cr fractionation during the life span of ^{53}Mn, which we interpret to represent the Mn/Cr fractionation associated with planetary differentiation and crust extraction (fig. S6).

The bulk ^{55}Mn/^{52}Cr ratio of Mars is estimated at 0.769 ± 0.136 (*33*), whereas the average ^{55}Mn/^{52}Cr ratio of the crust based on the composition of surface sediments (*34*) is 1.22 ± 0.27, consistent with the preferential partitioning of Mn in the crust during differentiation. Using these values and assuming average crustal and lithospheric mantle thicknesses of 50 and 500 km, respectively (*35*, *36*), mass balance requires that extraction of the primordial crust results in lowering the ^{55}Mn/^{52}Cr ratio of the residual mantle by ~6%. On the basis of these estimates, we show in Fig. 4 that the μ^{53}Cr values of the residual mantle and crustal endmembers can only be reproduced if Mn/Cr fractionation associated with primordial crust extraction occurred within 6.4 Ma after solar system formation. This age for primordial crust extraction is consistent with constraints from the

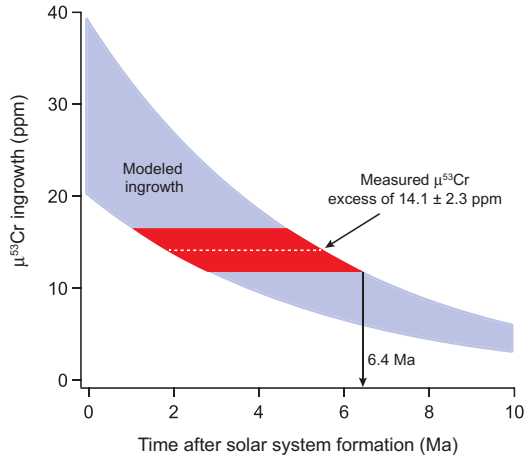

Fig. 4. Mn-Cr time evolution diagram. The time evolution of the $\mu^{53}Cr$ ingrowth, which represents the difference between the mantle and crustal reservoirs with modeled $^{55}Mn/^{52}Cr$ ratios of 0.724 ± 0.12 and 1.22 ± 0.27, respectively (see main text). We use a value of 0.769 ± 0.136 for the bulk $^{55}Mn/^{52}Cr$ ratio of Mars (*33*) and an initial solar system $^{53}Mn/^{55}Mn$ of 6.77×10^{-6} (*71*). The blue band reflects the range of $\mu^{53}Cr$ compositions considering the model uncertainty. The measured $\mu^{53}Cr$ excess of 14.1 ± 2.3 ppm represents the difference between the inferred mantle (ALHA 77005) and crustal (weighted mean of MIL 03346, MIL 090032, and NWA 7320) endmember compositions.

combined U-Pb ages and Hf isotope systematics of ancient Martian zircons that require primordial crust extraction within 20 Ma of solar system formation (*13*, *26*). We note that volatile-poor carbonaceous chondrites (i.e., CH, CV, CK, and CO), typified by $^{55}Mn/^{52}Cr$ ratios of 0.3 to 0.4, have $\mu^{53}Cr$ values comparable (*25*) to that observed here for the Martian mantle estimated by ALH 77005. These chondrites are inferred to have completed their accretion within the ~5-Ma protoplanetary disk lifetime, thereby supporting the time scale proposed here for the formation of the primordial Martian crust despite the uncertainties in the model parameters.

Implications for the past and current water inventory of Mars

During the late solidification of Mars, catastrophic outgassing of the mantle is predicted to have released a primordial surface water reservoir (*37*). Thus, Mars' cumulative water budget will consist of a primordial reservoir in addition to an exotic component derived from the impacting carbonaceous asteroids that we model to be CR chondrites (see Material and Methods and Supplementary Text). On the basis of the minimum impactor mass required to account for the exotic Cr in Mars' crust and assuming an average water to rock ratio of 0.1 for CR chondrites (*38*), we calculate that admixing of this material will result in a water inventory of ~307-m global equivalent layer (GEL) on the planet's surface, consistent with the lower range of estimates based on geomorphology (*39*). Because CR chondrites have a bulk D/H ratio enriched in deuterium (δD of 676 ± 46‰) (*40*) relative to the Martian mantle (δD <275‰) (*41*), using the mantle D/H value to model global atmospheric loss of H over time will yield inaccurate estimates because the D/H ratio of the cumulative water budget is a mixture of the primordial and exotic components. As the D/H ratio of the cumulative water budget will necessarily be more D-rich than the mantle value, it will result in an overestimation of the initial water inventory, implying that a lesser amount of water was lost by atmospheric escape. This requires the existence of a current reservoir of nonobservable water on Mars, the size of which depends on the proportion of primordial water relative to the exotic water component.

The current inventory of observable water on Mars is hosted by the polar layered deposits and corresponds to at least 20-m GEL (*42*, *43*). However, the existence of additional nonobservable water reservoirs has been proposed on the basis of the mismatch between the initial water inventory inferred from geomorphology and that based on the difference between the D/H value of the initial and current water inventory (*44*, *45*). Estimates for the quantity of nonobservable water on Mars today range from 100- to 1000-m GEL, a water mass that is hypothesized to be sequestered by crustal hydration (*45*) or, alternatively, stored as subsurface ice deposits (*46*). Assuming that Mars' initial water budget was solely derived from the impacting carbonaceous material, we calculate a minimum inventory of sequestered, nonobservable water corresponding to 185-m GEL, consistent with the lower range of estimates inferred from different approaches (*44*, *45*). However, increasing the proportion of primordial water relative to the exotic component will lead to a correspondingly larger current reservoir of nonobservable water (fig. S7). Although the size of the ancient surface water reservoir remains uncertain, our work emphasizes the need for a better understanding of the potential sources of ancient water to accurately model the hydrologic cycle on Mars, including the storage of water in the Martian crust.

Last, it has long been recognized that impacting carbonaceous asteroids and comets can provide a potential source of organic matter, including biologically relevant molecules such as amino acids, to planetary surfaces (*46*–*49*). Although the preservation rate of biologically relevant molecules is dependent on a number of factors such as impactor sizes and impact velocities (*50*), our results establish that exotic organic matter was delivered to the surface of Mars, providing an accessible inventory of carbon available for cycling between reservoirs during the early history of the planet. Thus, our results and interpretations are consistent with a meteoritic origin for the isotopically light carbon identified in ancient sediments from Gale crater (*51*, *52*).

MATERIALS AND METHODS

Sample selection, preparation, and digestion

We selected a total of 31 Martian meteorites, which includes 23 shergottites, 5 nakhlites, 1 chassignite (NWA 2737), 1 orthopyroxenite (ALH 84001), and the NWA 7533 regolith breccia. We selected our sample suite to include both falls and find and geochemically primitive (high Mg#) and evolved (low Mg#) lithologies. Fragments weighing between 20 and 200 mg were extracted from the available meteorites and crushed to powders using an agate mortar, and the powdered material was transferred to Teflon bombs for dissolution. Sample dissolution was achieved by means of concentrated HF and HNO_3 (2:1) at 140°C for 2 days, and after dry down, the solid residues were redissolved in 6 M HCl (at 140°C) for another 2 days to ensure complete digestion of fluorides and refractory phases such as chromite and spinel. All samples were visually inspected to ensure the lack of solid residue. Before chemical purification, a 10% aliquot was preserved for determination of elemental ratios, and the remainder of the samples were aliquoted equally for mass-dependent and mass-independent Cr isotope work.

Chromium purification and isotope analysis for determination of mass-independent compositions

The chemical purification used here for mass-independent work is based on a number previously described protocols (*53*–*56*) and detailed in full elsewhere (*25*). Briefly, we used a four-step column chemistry with typical yields ranging from ~95 to ~99% that involves anion, cation, and tetra-*n*-octyldiglycolamide (TODGA) resins. The first purification step is aimed at removing Fe on anion exchange resin (AG1-X8) in 6 M HCl. Before the second column chemistry using cation exchange resin (AG50W-X8) aimed at separating matrix elements (Mg, Ca, Al, Mn, and Ni), the samples were pretreated in 10 M HCl at >120°C to efficiently promote the formation of Cr^{3+}-Cl species, which have a low affinity for the cation exchanger (*56*). Subsequently, samples were loaded on the column in 0.5 M HCl and eluted in 0.5 M HNO_3. The recovered Cr cuts were then treated with 0.5 M HNO_3 + 0.6% H_2O_2 at room temperature for >1 day to promote the formation of Cr^{3+}. The third clean-up column involved cation exchange resin (AG50W-X8) and aimed at separating additional matrix elements (Na, Mg, K, Al, Fe, V, Ti, and other high–field strength elements) from Cr using 0.5 M HNO_3, 1 M HF, and 6 M HCl. Last, the fourth column uses TODGA resin to remove the residual Fe, V, and Ti in 8 M HCl. The total blank of our full purification protocol is <5 ng, which is negligible compared to the 10 to 20 μg of Cr processed through the columns. The final Cr solutions were dried down in concentrated HNO_3 three times to transform the acid media to a nitrate and remove residual organics from the resins.

The mass-independent Cr isotope compositions were determined using a Neptune Plus MC-ICPMS located at the Centre for Star and Planet Formation, Globe Institute, University of Copenhagen, Denmark. Detailed analytical and data reduction methods are described in earlier work (*25*, *55*). Each sample was measured by sample-standard bracketing using NIST SRM 979 as the reference Cr standard. Sample solutions of ~0.5 ppm were introduced to the plasma via an ESI Apex IR resulting in ^{52}Cr signals of 20 to 40 V at an uptake rate of ~0.06 ml/min. Each sample was measured 10 times. The mass-independent $^{53}Cr/^{52}Cr$ and $^{54}Cr/^{52}Cr$ ratios were normalized to a constant $^{50}Cr/^{52}Cr$ ratio of 0.051859 using the kinetic law. All the measured isotopic ratios are expressed relative to NIST SRM 979 in the μ notations as follows

$$\mu^{x}\mathrm{Cr} = \left(\frac{\left(\frac{^{x}\mathrm{Cr}}{^{52}\mathrm{Cr}}\right)_{\mathrm{sample}}}{\left(\frac{^{x}\mathrm{Cr}}{^{52}\mathrm{Cr}}\right)_{\mathrm{NIST\ SRM\ 979}}} - 1 \right) \times 1{,}000{,}000$$

where *x* is 53 or 54. The accuracy and external reproducibility of our measurements by repeated analyses of individual column-processed aliquots of the Allende meteorites and the DTS-1 terrestrial reference materials, which are reported by Zhu *et al.* (*25*) as the data obtained here and in the aforementioned work, were acquired in the same analytical session. On the basis of the Allende and DTS-1 data, summarized in table S2, we infer an external reproducibility of 4- and 7-ppm for the $\mu^{53}Cr$ and $\mu^{54}Cr$ values, respectively. Two duplicate sample digestions of Tissint and three duplicate digestions of Zagami yield $\mu^{53}Cr$ and $\mu^{54}Cr$ values that are within uncertainty, considering our inferred external reproducibility (table S1). A recent study of the mass-independent Cr isotope composition of Martian meteorites reports data for seven of the samples analyzed here, albeit at a lower precision, allowing for a comparison of the two datasets. All the $\mu^{53}Cr$ and $\mu^{54}Cr$ data are within error, considering the external reproducibility of 4 and 7 ppm, respectively, as well as the external reproducibility of 12 and 28 ppm reported by Kruijer *et al.* (*19*) (fig. S8).

Chromium purification and isotope analysis for determination of mass-dependent compositions

The mass-dependent Cr isotope compositions were determined using double-spike techniques using the approach outlined by Sossi *et al.* (*57*) and conducted in a different laboratory (Institut de Physique du Globe de Paris) to avoid potential contamination of the unspiked aliquots from the ^{50}Cr-^{54}Cr double spike. First, the adequate amount of the ^{50}Cr-^{54}Cr double spike, which corresponds to 28% of the Cr content endemic to the samples, was added to the aliquots reserved for double-spike work. The samples were fluxed in closed beakers at 120°C overnight. Chromium from the spiked samples was purified via a two-step cation exchange chromatography adapted from (*53*) and described elsewhere (*58*). The purified Cr cuts were dried down and treated with concentrated HNO_3 to convert the samples to nitrate form and eliminate any residual organics from the resin and, lastly, dissolved in 2% HNO_3 for isotope analysis.

The Cr stable isotope composition of the purified samples were measured on a Neptune Plus MC-ICPMS housed at the Institut de Physique du Globe de Paris on the basis of previously described protocols (*57*). The stable isotope compositions are reported relative to NIST SRM 979 in the δ notation as follows

$$\delta^{53}\mathrm{Cr}(‰) = \left(\frac{\left(\frac{^{53}\mathrm{Cr}}{^{52}\mathrm{Cr}}\right)_{\mathrm{sample}}}{\left(\frac{^{53}\mathrm{Cr}}{^{52}\mathrm{Cr}}\right)_{\mathrm{NIST\ SRM\ 979}}} - 1 \right) \times 1000$$

Samples were measured at least two times, and the quoted uncertainty reflects the 2SD. We used the reported mass-independent composition in the spike deconvolution algorithm to determine the $\delta^{53}Cr$ values. However, given the small range of $\mu^{53}Cr$ and $\mu^{54}Cr$ values for our samples, using the measured mass-independent composition results in a $\delta^{53}Cr$ shift that is within the typical uncertainty of the stable isotope measurements. The stable isotope data reported here were acquired in the framework of a large analytical session that included the determination of the $\delta^{53}Cr$ values of several chondrites (*58*). The reference materials analyzed in this session to test for data accuracy include BHVO-2, PCC-1, and DTS-1 and are summarized in table S3 and compare favorably with literature data. Last, the value we report for Nakhla is identical to that reported in earlier work (*59*), confirming the accuracy of the data.

Samarium purification and isotope analysis

We selected five Martian meteorites covering the range of observed $\mu^{53}Cr$ and $\mu^{54}Cr$ values to investigate whether the variable Cr isotope data could be accounted for by spallogenic effects. Powders of selected meteorites weighing 40 to 500 mg were dissolved in concentrated HF-HNO_3 mixture at 150°C on a hotplate for 2 days. Repeated treatment with concentrated aqua regia and 6 M HCl followed HF-HNO_3 digestion until a clear solution was obtained. Samarium was purified from the ample matrix in a two-step procedure. The rare earth elements (REE) were first isolated as a group on a cation exchange column following the procedure described by Saji *et al.* (*21*). We used a 2-ml capacity Bio-Rad column filled with AG50W-X8

(200 to 400 mesh) resin, and high–field strength elements were first washed off from the column with 1 M HF. The remaining major elements were removed by elution with 2 M HNO_3, and the REE fraction was lastly eluted with 6 M HNO_3. Samarium was subsequently separated from other REEs using a Dionex equipped with a fraction collector, where samples were eluted through a LN2-spec column by elution with 0.2 M HNO_3. Residual Nd interference levels after a single pass of LN2 resulted in corrections of around 10,000 ppm on ^{150}Sm. To limit this, we passed the Sm-cut a second time through the LN2-spec column, at which point the final correction from ^{150}Nd interference was on the order of a few hundred parts per million and, thus, inconsequential for the accuracy of the ^{150}Sm/^{152}Sm ratio within the stated uncertainties. Gadolinium interference levels on ^{152}Sm used for internal mass bias correction were significantly less than 10 ppm.

Sm isotopes were measured on a Neptune Plus MC-ICPMS instrument at the Centre for Star and Planet Formation (University of Copenhagen) by sample-standard bracketing using an Aristar Sm ICPMS solution as a bracketing standard, and isotope data are reported as parts per million deviations of the ^{150}Sm/^{152}Sm ratio from the standard, normalized to constant ^{147}Nd/^{152}Nd = 0.56081. Samples were dissolved in 2% HNO_3 and introduced into the plasma source via an ESI Apex IR at an aspiration rate of 0.1 ml/min. Between 2 and 70 ng of Sm was analyzed for the individual samples dissolved in 3 ml, and signal intensities on ^{149}Sm ranged from 0.12 to 4.65 V. A single analysis consisted of 55 cycles with an integration interval of 8.34 s, and each sample was analyzed three times. Reported uncertainties are the 2SD of the three individual analyses, and uncertainties are primarily controlled by the available material for analysis.

Determination of elemental ratios

An unprocessed aliquot from the original digestion of the Martian meteorites analyzed here was preserved for elemental ratio determination. The ^{55}Mn/^{52}Cr ratio of all samples were determined using a Neptune Plus MC-ICPMS located at the Institut de Physique du Globe de Paris (Paris, France) by the sample-standard bracketing approach using gravimetrically prepared standards of known ^{55}Mn/^{52}Cr ratio, which provides an accuracy of ~5% (*25*). Elemental ratios for major and trace elements were determined on the same aliquots using either an Agilent 7900 ICPMS (Institut de Physique du Globe de Paris) or an iCap ICPMS (Centre for Star and Planet Formation) by the sample-standard bracketing approach and using gravimetrically prepared solution of known concentration as the bracketing standards. This method ensures an accuracy of 10% for all elemental ratios reported here.

Determination of the mass of exotic material delivered to Mars by impacts

As dynamical models suggest that the influx of outer solar system material to the terrestrial planet formation region occurred early (*3*, *29*), we consider the earliest impactor populations on Mars within hundreds of million years after the planet's formation. The observed impact basin populations on the Martian surface provides a lower limit to constrain the total mass of accreted materials from chondritic impactors. The first 400 Ma of Mars do not have a well-preserved cratering record (*60*), and the extrapolated impactor population for this period is model dependent (*29*, *61*). Conservatively, we consider the observational evidence for early impactors on Mars from buried impact basins to the Martian dichotomy. In the first scenario, we include only the oldest large impact basins from the work of Frey (*32*) with a Crater Ray Age greater than 2 (excluding Hellas, Argyre, and Isidis). The selected basins likely formed during the pre-Noachian to Noachian period (4.4 to 4.1 Ga). In the second scenario, we consider the possible giant impact that created the Martian dichotomy, predating the current Martian surface (*62*, *63*), a possible major event where chondritic materials were delivered to the Martian crust and mantle. These two cases provide the best estimate for the known population of pre-Noachian impactor flux. To calculate the impactor sizes for large basins on Mars, we used the following scaling relationship (*64*)

$$D_t = D_*^{0.15} D_f^{0.85}$$

Here, D_t is the transient crater diameter, D_* is the simple-to-complex transition diameter (~7 km on Mars), and D_f is the final crater diameter. The transient crater diameter, D_{tr}, is then translated to D_{tc} with a factor of 1.2 (*65*). Scaling relationship between impactor kinetic energy and transient cavity size gives

$$D_t = \frac{2\rho_t^{0.11} R^{0.13} E^{0.22} (\sin\theta)^{1/3}}{\rho_p^{1/3} g^{0.22}}$$

where we take ρ_p (density of projectile) = 2835 kg m^{-3}, E (impactor kinetic energy) = $\left(\frac{2}{3}\right)\pi R^3 \rho_m v^2$, v (average impactor velocity) = 10 km s^{-1}, θ (most probable impact angle) = 45°, ρ_p (density of basaltic target material) = 3000 kg m^{-3}, and g (gravity) = 3.71 m s^{-2}. The density is estimated considering the average density of CR chondrites (3.05×10^3 kg m^{-3}) (*66*) with 10% ice component, consistent with the inferred water/rock ratio of CR chondrites (*38*). For the dichotomy-forming impact, we chose to use the output from a previous hydrocode simulation that estimated the impactor size to be 1600 km in diameter (*67*) under the assumptions of relevant impact velocity and density.

The mass of the impactor materials is calculated as $M = 4/3\pi(D_p/2)^3 \rho_p$, assuming a constant density of the projectile. Notably, the amount of material accreted to the planet is dominated by the largest impactors ($M \sim R^3$), so the dichotomy-forming impactor is an order of magnitude more important in total mass from impactors that from smaller impact basins and craters.

Assuming an endmember composition of Cr isotope for CR chondrites (μ^{54}Cr = 128 ± 4 ppm) and Martian mantle (μ^{54}Cr = −33 ppm), 24% admixing of chondritic materials is required in the Martian crust to explain the observed endmember crustal composition from Martian meteorites (μ^{54}Cr = 8.3 ppm, i.e., 6.8 + 1.5 ppm). For smaller impacts, most of the impactor materials are either vaporized or enter the melt pool (*68*). Therefore, we expect a greater concentration of anomalous chromium composition close to the Martian surface, later reworked by small impacts throughout Martian history. The upper 8 to 12 km of the Martian crust has low seismic velocity, possibly corresponding to a highly fractured or disrupted layer (*69*). We show here that the first 4 km thoroughly mixed with chondritic materials from the basin-forming impactors could explain the endmember Cr signature in the Martian crust. Including the dichotomy-forming impact extends the depth of mixing to that of the entire crust. Hence, admixing of chondritic material to the first 4 km represents a minimum estimate. We discuss in the Supplementary Materials that the CR chondrite provides the most likely endmember

for the impacting material, consistent with both cosmochemical observations (*30*, *31*) and dynamical models (*29*). However, if we consider CO chondrites that have the least anomalous ^{54}Cr composition [μ^{54}Cr = 50 ppm (*25*)] as an alternative endmember, then 49% impactor material is expected in the final mixtures, which requires either a restricted mixing zone (2 km for the basin-forming impactors and a thin Mars crust for dichotomy-forming impact) or twice the amount of impactor mass than assumed here (fig. S9). Thus, our estimate of the amount of exotic carbonaceous material delivered to Mars on the basis of CR chondrites represents a strict minimum. The scaling and mass balance presented here assume that the impact-modified Martian crust and mantle are well-mixed reservoirs. The heterogeneous nature of impact processes could result in local variations in the concentration of chondritic materials, which, in principle, may require a smaller impactor flux to account for the observed distribution of chromium isotopic composition of Martian meteorites. However, the suggestion that shergottite magmas originate from distinct mantle sources that later experienced fractional crystallization in different crustal magma chambers (*70*) supports our proposal that the ^{54}Cr-enriched signal identified here reflects a crustal signature.

SUPPLEMENTARY MATERIALS

Supplementary material for this article is available at https://science.org/doi/10.1126/sciadv.abp8415

View/request a protocol for this paper from *Bio-protocol*.

REFERENCES AND NOTES

1. G. Neukum, B. A. Ivanov, W. K. Hartmann, Cratering records in the inner Solar System in relation to the lunar reference system. *Space Sci. Rev.* **96**, 55–86 (2001).
2. W. F. Bottke, M. D. Norman, The late heavy bombardment. *Annu. Rev. Earth Planet. Sci.* **45**, 619–647 (2017).
3. D. Nesvorný, D. Vokrouhlický, W. F. Bottke, H. F. Levison, Evidence for very early migration of the Solar System planets from the Patroclus–Menoetius binary Jupiter Trojan. *Nat. Astron.* **2**, 878–882 (2018).
4. F. Albarède, Volatile accretion history of the terrestrial planets and dynamic implications. *Nature* **461**, 1227–1233 (2009).
5. Z. Wang, H. Becker, Ratios of S, Se and Te in the silicate Earth require a volatile-rich late veneer. *Nature* **499**, 328–331 (2013).
6. L. Piani, Y. Marrocchi, T. Rigaudier, L. G. Vacher, D. Thomassin, B. Marty, Earth's water may have been inherited from material similar to enstatite chondrite meteorites. *Science* **369**, 1110–1113 (2020).
7. N. Dauphas, A. Pourmand, Hf–W–Th evidence for rapid growth of Mars and its status as a planetary embryo. *Nature* **473**, 489–492 (2011).
8. A. Johansen, M. M. Mac Low, P. Lacerda, M. Bizzarro, Growth of asteroids, planetary embryos, and Kuiper belt objects by chondrule accretion. *Sci. Adv.* **1**, e1500109 (2015).
9. M. Maurice, N. Tosi, H. Samuel, A. C. Plesa, C. Hüttig, D. Breuer, Onset of solid-state mantle convection and mixing during magma ocean solidification. *J. Geophys. Res.* **122**, 577–598 (2017).
10. M. Grott, D. Baratoux, E. Hauber, V. Sautter, J. Mustard, O. Gasnault, S. W. Ruff, S.-I. Karato, V. Debaille, M. Knapmeyer, F. Sohl, T. Van Hoolst, D. Breuer, A. Morschhauser, M. J. Toplis, Long-term evolution of the martian crust-mantle system. *Space Sci. Rev.* **174**, 49–111 (2013).
11. L. E. Borg, L. E. Nyquist, H. Wiesmann, Y. Reese, Constraints on the petrogenesis of Martian meteorites from the Rb–Sr and Sm–Nd isotopic systematics of the lherzolitic shergottites ALH77005 and LEW88516. *Geochim. Cosmochim. Acta* **66**, 2037–2053 (2002).
12. H. H. B. Franz, S.-T. Kim, J. Farquhar, J. M. D. Day, R. C. Economos, K. D. McKeegan, A. K. Schmitt, A. J. Irving, J. Hoek, J. Dottin III, Isotopic links between atmospheric chemistry and the deep sulphur cycle on Mars. *Nature* **508**, 364–368 (2014).
13. M. M. Costa, N. K. Jensen, L. C. Bouvier, J. N. Connelly, T. Mikouchi, M. S. A. Horstwood, J.-P. Suuronen, F. Moynier, Z. Deng, A. Agranier, L. A. J. Martin, T. E. Johnson, A. A. Nemchin, M. Bizzarro, The internal structure and geodynamics of Mars inferred from a 4.2-Gyr zircon record. *Proc. Natl. Acad. Sci. U.S.A.* **117**, 30973–30979 (2020).
14. Z. Deng, F. Moynier, J. Villeneuve, N. K. Jensen, D. Liu, P. Cartigny, T. Mikouchi, J. Siebert, A. Agranier, M. Chaussidon, M. Bizzarro, Early oxidation of the martian crust triggered by impacts. *Sci. Adv.* **6**, eabc4941 (2020).
15. S. C. Werner, The early Martian evolution—Constraints from basin formation ages. *Icarus* **195**, 45–60 (2008).
16. M. D. Bjorkman, K. A. Holsapple, Velocity scaling impact melt volume. *Int. J. Impact Eng.* **5**, 155–163 (1987).
17. N. Dauphas, E. A. Schauble, Mass fractionation laws, mass-independent effects, and isotopic anomalies. *Annu. Rev. Earth Planet. Sci.* **44**, 709–783 (2016).
18. A. Trinquier, J.-L. Birck, C. J. Allègre, Widespread ^{54}Cr heterogeneity in the inner solar system. *Astrophys. J.* **655**, 1179–1185 (2007).
19. T. S. Kruijer, L. E. Borg, J. Wimpenny, C. K. Sio, Onset of magma ocean solidification on Mars inferred from Mn-Cr chronometry. *Earth Planet. Sci. Lett.* **542**, 116315 (2020).
20. N. S. Saji, D. Wielandt, J. C. Holst, M. Bizzarro, Solar system Nd isotope heterogeneity: Insights into nucleosynthetic components and protoplanetary disk evolution. *Geochim. Cosmochim. Acta* **281**, 135–148 (2020).
21. N. S. Saji, M. Schiller, J. C. Holst, M. Bizzarro, Isotope dichotomy from solar protoplanetary disk processing of ^{150}Nd-rich stellar ejecta. *Astrophys. J. Lett.* **919**, L8 (2021).
22. H. Y. McSween, Petrology on mars. *Am. Mineral.* **100**, 2380–2395 (2015).
23. J. Shen, J. Xia, L. Qin, R. W. Carlson, S. Huang, R. T. Helz, T. D. Mock, Stable chromium isotope fractionation during magmatic differentiation: Insights from Hawaiian basalts and implications for planetary redox conditions. *Geochim. Cosmochim. Acta* **278**, 289–304 (2020).
24. N. Mari, A. Riches, L. J. Hallis, Y. Marrocchi, J. Villeneuve, P. Gleissner, H. Becker, M. R. Lee, Syneruptive incorporation of martian surface sulphur in the nakhlite lava flows revealed by S and Os isotopes and highly siderophile elements: Implication for mantle sources in Mars. *Geochim. Cosmochim. Acta* **266**, 416–434 (2019).
25. K. Zhu, F. Moynier, M. Schiller, C. M. O.'. D. Alexander, J. Davidson, D. L. Schrader, E. van Kooten, M. Bizzarro, Chromium isotopic insights into the origin of chondrite parent bodies and the early terrestrial volatile depletion. *Geochim. Cosmochim. Acta* **301**, 158–186 (2021).
26. L. C. Bouvier, M. M. Costa, J. N. Connelly, N. K. Jensen, D. Wielandt, M. Storey, A. A. Nemchin, M. J. Whitehouse, J. F. Snape, J. J. Bellucci, F. Moynier, A. Agranier, B. Gueguen, M. Schönbächler, M. Bizzarro, Evidence for extremely rapid magma ocean crystallization and crust formation on Mars. *Nature* **558**, 586–589 (2018).
27. L E. Borg, G. A. Brennecka, S. J. K. Symes, Accretion timescale and impact history of Mars deduced from the isotopic systematics of martian meteorites. *Geochim. Cosmochim. Acta* **175**, 150–167, 150–167 (2016).
28. F. Nimmo, S. Hart, D. Korycansky, C. B. Agnor, Implications of an impact origin for the martian hemispheric dichotomy. *Nature* **453**, 1220–1223 (2008).
29. R. Brasser, S. Werner, S. J. Mojzsis, Impact bombardment chronology of the terrestrial planets from 4.5 Ga to 3.5 Ga. *Icarus* **338**, 113514 (2020).
30. E. M. M. E. Van Kooten, D. Wielandt, M. Schiller, K. Nagashima, A. Thomen, K. K. Larsen, M. B. Olsen, Å. Nordlund, A. N. Krot, M. Bizzarro, Isotopic evidence for primordial molecular cloud material in metal-rich carbonaceous chondrites. *Proc. Natl. Acad. Sci. U.S.A.* **113**, 2011–2016 (2016).
31. T. Obase, D. Nakashima, J. Choi, Y. Enokido, M. Matsumoto, T. Nakamura, Water-susceptible primordial noble gas components in less-altered CR chondrites: A possible link to cometary materials. *Geochim. Cosmochim. Acta* **312**, 75–105 (2021).
32. H. Frey, Ages of very large impact basins on Mars: Implications for the late heavy bombardment in the inner solar system. *Geophys. Res. Lett.* **35**, L13203 (2008).
33. G. J. Taylor, The bulk composition of Mars. *Chem. Erde* **73**, 401–420 (2013).
34. S. M. McLennan, J. P. Grotzinger, J. A. Hurowitz, N. J. Tosca, The sedimentary cycle on early mars. *Annu. Rev. Earth Planet. Sci.* **47**, 91–118 (2019).
35. B. Knapmeyer-Endrun, M. P. Panning, F. Bissig, R. Joshi, A. Khan, D. Kim, V. Lekić, B. Tauzin, S. Tharimena, M. Plasman, N. Compaire, R. F. Garcia, L. Margerin, M. Schimmel, É. Stutzmann, N. Schmerr, E. Bozdağ, A. C. Plesa, M. A. Wieczorek, A. Broquet, D. Antonangeli, S. M. McLennan, H. Samuel, C. Michaut, L. Pan, S. E. Smrekar, C. L. Johnson, N. Brinkman, A. Mittelholz, A. Rivoldini, P. M. Davis, P. Lognonné, B. Pinot, J. R. Scholz, S. Stähler, M. Knapmeyer, M. van Driel, D. Giardini, W. B. Banerdt, Thickness and structure of the martian crust from InSight seismic data. *Science* **373**, 438–443 (2021).
36. A. Khan, S. Ceylan, M. van Driel, D. Giardini, P. Lognonné, H. Samuel, N. C. Schmerr, S. C. Stähler, A. C. Duran, Q. Huang, D. Kim, A. Broquet, C. Charalambous, J. F. Clinton, P. M. Davis, M. Drilleau, F. Karakostas, V. Lekic, S. M. McLennan, R. R. Maguire, C. Michaut, M. P. Panning, W. T. Pike, B. Pinot, M. Plasman, J. R. Scholz, R. Widmer-Schnidrig, T. Spohn, S. E. Smrekar, W. B. Banerdt, Upper mantle structure of Mars from InSight seismic data. *Science* **373**, 434–438 (2021).
37. L. T. Elkins-Tanton, Linked magma ocean solidification and atmospheric growth for Earth and Mars. *Earth Planet. Sci. Lett.* **271**, 181–191 (2008).
38. C. M. O'. D. Alexander, Quantitative models for the elemental and isotopic fractionations in chondrites: The carbonaceous chondrites. *Geochim. Cosmochim. Acta* **254**, 277–309 (2019).
39. G. Di Achille, B. Hynek, Ancient ocean on Mars supported by global distribution of deltas and valleys. *Nat. Geosci.* **3**, 459–463 (2010).

40. C. M. O'. D. Alexander, R. Bowden, M. L. Fogel, K. T. Howard, C. D. K. Herd, L. R. Nittler, The provenances of asteroids, and their contributions to the volatile inventories of the terrestrial planets. *Science* **337**, 721–723 (2012).
41. T. Usui, C. M. O'. D. Alexander, J. Wang, J. I. Simon, J. H. Jones, Origin of water and mantle–Crust interactions on Mars inferred from hydrogen isotopes and volatile element abundances of olivine-hosted melt inclusions of primitive shergottites. *Earth Planet. Sci. Lett.* **357**, 119–129 (2012).
42. M. T. Zuber, D. E. Smith, S. C. Solomon, J. B. Abshire, R. S. Afzal, O. Aharonson, K. Fishbaugh, P. G. Ford, H. V. Frey, J. B. Garvin, J. W. Head, A. B. Ivanov, C. L. Johnson, D. O. Muhleman, G. A. Neumann, G. H. Pettengill, R. J. Phillips, X. Sun, H. J. Zwally, W. B. Banerdt, T. C. Duxbury, Observations of the north polar region of Mars from the Mars orbiter laser altimeter. *Science* **282**, 2053–2060 (1998).
43. J. J. Plaut, G. Picardi, A. Safaeinili, A. B. Ivanov, S. M. Milkovich, A. Cicchetti, W. Kofman, J. ... Mouginot, W. M. Farrell, R. J. Phillips, S. M. Clifford, A. Frigeri, R. Orosei, C. Federico, I. P. Williams, D. A. Gurnett, E. Nielsen, T. Hagfors, E. Heggy, E. R. Stofan, D. Plettemeier, T. R. Watters, C. J. Leuschen, P. Edenhofer, Subsurface radar sounding of the south polar layered deposits of Mars. *Science* **316**, 92–95 (2007).
44. H. Kurokawa, M. Sato, M. Ushioda, T. Matsuyama, R. Moriwaki, J. M. Dohmd, T. Usui, Evolution of water reservoirs on Mars: Constraints from hydrogen isotopes in martian meteorites. *Earth Planet. Sci. Lett.* **394**, 179–185 (2014).
45. E. L. Scheller, B. L. Ehlmann, H. Renyu, D. J. Adams, Y. L. Yung, Long-term drying of Mars by sequestration of ocean-scale volumes of water in the crust. *Science* **372**, 56–162 (2021).
46. C. Chyba, The cometary contribution to the oceans of primitive Earth. *Nature* **330**, 632–635 (1987).
47. E. Anders, Pre-biotic organic matter from comets and asteroids. *Nature* **342**, 255–257 (1989).
48. C. F. Chyba, P. J. Thomas, L. Brookshaw, C. Sagan, Cometary delivery of organic molecules to the early Earth. *Science* **249**, 366–373 (1990).
49. L. Rotelli, J. Trigo-Rodríguez, C. Moyano-Cambero, E. Carota, L. Botta, E. Di Mauro, The key role of meteorites in the formation of relevant prebiotic molecules in a formamide/water environment. *Sci. Rep.* **6**, 38888 (2016).
50. E. Pierazzo, C. Chyba, Impact delivery of prebiotic organic matter to planetary surfaces, in *Comets and the Origin and Evolution of Life*, P. J. Thomas, R. D. Hicks, C. F. Chyba, C. P. McKay, Eds. (Advances in Astrobiology and Biogeophysics, Springer, Berlin, Heidelberg, 2006).
51. H. B. Franz, P. R. Mahaffy, C. R. Webster, G. J. Flesch, E. Raaen, C. Freissinet, S. K. Atreya, C. H. House, A. C. McAdam, C. A. Knudson, P. D. Archer Jr., J. C. Stern, A. Steele, B. Sutter, J. L. Eigenbrode, D. P. Glavin, J. M. T. Lewis, C. A. Malespin, M. Millan, D. W. Ming, R. Navarro-González, R. E. Summons, Indigenous and exogenous organics and surface–Atmosphere cycling inferred from carbon and oxygen isotopes at Gale crater. *Nat. Astron.* **4**, 526–532 (2020).
52. J. C. Stern, C. A. Malespin, J. L. Eigenbrode, C. R. Webster, G. Flesch, H. B. Franz, H. V. Graham, C. H. House, B. Sutter, P. D. Archer Jr., A. E. Hofmann, A. C. McAdam, D. W. Ming, R. Navarro-Gonzalez, A. Steele, C. Freissinet, P. R. Mahaffy, Organic carbon concentrations in 3.5-billion-year-old lacustrine mudstones of Mars. *Proc. Natl. Acad. Sci. U.S.A.* **119**, e2201139119 (2022).
53. A. Trinquier, J.-L. Birck, C. J. Allègre, High-precision analysis of chromium isotopes in terrestrial and meteorite samples by thermal ionization mass spectrometry. *J. Anal. At. Spectrom* **23**, 1565–1574 (2008).
54. M. Bizzarro, C. Paton, K. Larsen, M. Schiller, A. Trinquier, D. Ulfbeck, High-precision Mg-isotope measurements of terrestrial and extraterrestrial material by HR-MC-ICPMS – Implications for the relative and absolute Mg-isotope composition of the bulk silicate Earth. *J. Anal. At. Spectrom* **26**, 565–577 (2011).
55. M. Schiller, E. Van Kooten, J. C. Holst, M. B. Olsen, M. Bizzarro, Precise measurement of chromium isotopes by MC-ICPMS. *J. Anal. At. Spectrom* **29**, 1406–1416 (2014).
56. K. K. Larsen, D. Wielandt, M. Schiller, M. Bizzarro, Chromatographic speciation of Cr(III)-species, inter-species equilibrium isotope fractionation and improved chemical purification strategies for high-precision isotope analysis. *J. Chromatogr. A* **1443**, 162–174 (2016).
57. P. A. Sossi, F. Moynier, K. van Zuilen, Volatile loss following cooling and accretion of the Moon revealed by chromium isotopes. *Proc. Natl. Acad. Sci. U.S.A.* **115**, 10920–10925 (2018).
58. J. Davidson, D. L. Schrader, J.-M. Zhu, G.-L. Wu, M. Schiller, M. Bizzarro, H. Becker, Chromium stable isotope panorama of chondrites and implications for earth early accretion. *Astrophys. J.* **923**, 94 (2021).
59. P. Bonnand, H. M. Williams, I. J. Parkinson, B. J. Wood, A. N. Halliday, Stable chromium isotopic composition of meteorites and metal-silicate experiments: Implications for fractionation during core formation. *Earth Planet. Sci. Lett.* **435**, 14–21 (2016).
60. B. A. Ivanov, Mars/Moon Cratering Rate Ratio Estimates, in *Chronology and Evolution of Mars*, R. Kallenbach, J. Geiss, W. K. Hartmann, Eds. (Springer Netherlands, 2001), vol. 12, pp. 87–104.
61. S. C. Werner, In situ calibration of the Martian cratering chronology. *Meteorit. Planet. Sci.* **54**, 1182–1193 (2019).
62. H. V. Frey, J. H. Roark, K. M. Shockey, E. L. Frey, S. E. Sakimoto, Ancient lowlands on Mars. *Geophys. Res. Lett.* **29**, 22-1–22-4 (2002).
63. H. V. Frey, Impact constraints on the age and origin of the lowlands of Mars. *Geophys. Res. Lett.* **33**, L08S02 (2006).
64. S. K. Croft, The scaling of complex craters. *J. Geophys. Res. Solid Earth* **90**, C828–C842 (1985).
65. R. J. Pike, Size-dependence in the shape of fresh impact craters on the Moon, in *Impact and explosion cratering: Planetary and terrestrial implications* (1977), pp. 489–509.
66. R. J. Macke, G. J. Consolmagno, D. T. Britt, Density, porosity, and magnetic susceptibility of carbonaceous chondrites. *Meteorit. Planet. Sci.* **46**, 1842–1862 (2011).
67. M. M. Marinova, O. Aharonson, E. Asphaug, Mega-impact formation of the Mars hemispheric dichotomy. *Nature* **453**, 1216–1219 (2008).
68. P. H. Schultz, S. Sugita, Fate of the Chicxulub impactor, in Lunar and Planetary Science Conference (1997) vol. XXVIII pp. 1792.
69. P. Lognonné, W. B. Banerdt, W. T. Pike, D. Giardini, U. Christensen, R. F. Garcia, T. Kawamura, S. Kedar, B. Knapmeyer-Endrun, L. Margerin, F. Nimmo, M. Panning, B. Tauzin, J. R. Scholz, D. Antonangeli, S. Barkaoui, E. Beucler, F. Bissig, N. Brinkman, M. Calvet, S. Ceylan, C. Charalambous, P. Davis, M. van Driel, M. Drilleau, L. Fayon, R. Joshi, B. Kenda, A. Khan, M. Knapmeyer, V. Lekic, J. McClean, D. Mimoun, N. Murdoch, L. Pan, C. Perrin, B. Pinot, L. Pou, S. Menina, S. Rodriguez, C. Schmelzbach, N. Schmerr, D. Sollberger, A. Spiga, S. Stähler, A. Stott, E. Stutzmann, S. Tharimena, R. Widmer-Schnidrig, F. Andersson, V. Ansan, C. Beghein, M. Böse, E. Bozdag, J. Clinton, I. Daubar, P. Delage, N. Fuji, M. Golombek, M. Grott, A. Horleston, K. Hurst, J. Irving, A. Jacob, J. Knollenberg, S. Krasner, C. Krause, R. Lorenz, C. Michaut, R. Myhill, T. Nissen-Meyer, J. ten Pierick, A. C. Plesa, C. Quantin-Nataf, J. Robertsson, L. Rochas, M. Schimmel, S. Smrekar, T. Spohn, N. Teanby, J. Tromp, J. Vallade, N. Verdier, C. Vrettos, R. Weber, D. Banfield, E. Barrett, M. Bierwirth, S. Calcutt, N. Compaire, C. L. Johnson, D. Mance, F. Euchner, L. Kerjean, G. Mainsant, A. Mocquet, J. A. Rodriguez Manfredi, G. Pont, P. Laudet, T. Nebut, S. de Raucourt, O. Robert, C. T. Russell, A. Sylvestre-Baron, S. Tillier, T. Warren, M. Wieczorek, C. Yana, P. Zweifel, Constraints on the shallow elastic and anelastic structure of Mars from InSight seismic data. *Nat. Geosci.* **13**, 213–220 (2020).
70. S. J. K. Symes, L. E. Borg, C. K. Schearer, A. J. Irving, The age of the martian meteorite Northwest Africa 1195 and the differentiation history of the shergottites. *Geochim. Cosmochim. Acta* **72**, 1696–1710 (2008).
71. D. P. Glavin, A. Kubny, E. Jagoutz, G. W. Lugmair, Mn-Cr isotope systematics of the D'Orbigny angrite. *Meteorit. Planet. Sci.* **39**, 693–700 (2004).
72. G. Briani, M. Gounelle, Y. Marrocchi, S. Mostefaoui, H. Leroux, E. Quirico, A. Meibom, Pristine extraterrestrial material with unprecedented nitrogen isotopic variation. *Proc. Natl. Acad. Sci. U.S.A.* **106**, 10522–10527 (2009).
73. L. Bonal, G. R. Huss, A. N. Krot, K. Nagashima, Highly ^{15}N-enriched chondritic clasts in the CB/CH-like meteorite Isheyevo. *Geochim. Cosmochim. Acta* **74**, 6590–6609 (2009).
74. S. D. Rodgers, S. B. Charnley, Nitrogen superfractionation in dense cloud cores. *Mon Not. R Astron. Soc.* **385**, L48–L52 (2008).
75. S. F. Wampfler, J. K. Jørgensen, M. Bizzarro, S. E. Bisschop, Observations of nitrogen isotope fractionation in deeply embedded protostars. *Astron. Astrophys.* **572**, A24 (2014).
76. A. N. Krot, A. Meibom, M. K. Weinberg, K. Keil, The CR chondrite clan: Implications for early solar system processes. *Meteorit. Planet. Sci.* **37**, 1451–1490 (2002).
77. R. C. Ogliore, G. R. Huss, K. Nagashima, A. L. Butterworth, Z. Gainsforth, J. Stodolna, A. J. Westphal, D. Joswiak, T. Tyliszczak, Incorporation of a late-forming chondrule into comet wild 2. *Astrophys. J. Lett.* **745**, L19–L23 (2012).
78. D. Nakashima, T. Ushikubo, D. J. Joswiak, D. E. Brownlee, G. Matrajt, M. K. Weisberg, M. E. Zolensky, N. T. Kita, Oxygen isotopes in crystalline silicates of comet Wild 2: A comparison of oxygen isotope systematics between Wild 2 particles and chondritic materials. *Earth Planet. Sci. Lett.* **357**, 355–365 (2012).
79. D. R. Frank, M. E. Zolensky, L. Le, Olivine in terminal particles of Stardust aerogel tracks and analogous grains in chondrite matrix. *Geochim. Cosmochim. Acta* **142**, 240–259 (2014).
80. C. Defouilloy, D. Nakashima, D. J. Joswiak, D. E. Brownlee, T. J. Tenner, N. T. Kita, Origin of crystalline silicates from Comet 81P/Wild 2: Combined study on their oxygen isotopes and mineral chemistry. *Earth Planet. Sci. Lett.* **465**, 145–154 (2017).
81. L. R. Nittler, R. M. Stroud, J. M. Trigo-Rodríguez, B. T. De Gregorio, C. M. O'. D. Alexander, J. Davidson, C. E. Moyano-Cambero, S. Tanbakouei, A cometary building block in a primitive asteroidal meteorite. *Nat. Astron* **3**, 659–666 (2019).
82. E. van Kooten, M. Schiller, F. Moynier, A. Johansen, T. Haugbølle, M. Bizzarro, Hybrid accretion of carbonaceous chondrites by radial transport across the jupiter barrier. *Astrophys. J.* **910**, 70 (2021).
83. M. B. Olsen, D. Wielandt, M. Schiller, E. M. M. E. Van Kooten, M. Bizzarro, Magnesium and ^{54}Cr isotope compositions of carbonaceous chondrite chondrules—Insights into early disk processes. *Geochim. Cosmochim. Acta* **191**, 118–138 (2016).

84. R. W. Nicklas, J. M. D. Day, Z. Vaci, A. Udry, Y. Liu, K. T. Tait, Uniform oxygen fugacity of shergottite mantle sources and an oxidized martian lithosphere. *Earth Planet. Sci. Lett.* **564**, 116876 (2021).
85. R. R. Rahib, A. Udry, G. H. Howarth, J. Gross, M. Paquet, L. M. Combs, D. L. Laczniak, J. M. D. Day, Mantle source to near-surface emplacement of enriched and intermediate poikilitic shergottites in Mars. *Geochim. Cosmochim. Acta* **266**, 463–496 (2019).
86. Z. Wang, W. Tian, Y. Di, New temperature and oxygen fugacity data of Martian nakhlite from Northwest Africa (NWA) 5790 and implications for shallow sulphur degassing. *Earth Planets Space* **73**, 164 (2021).
87. W. A. Bohrson, F. J. Spera, M. S. Ghiorso, G. A. Brown, J. B. Creamer, A. Mafield, Thermodynamic model for energy-constrained open-system evolution of crustal magma bodies undergoing simultaneous recharge, assimilation and crystallization: The magma chamber simulator. *J. Petrol.* **55**, 1685–1717 (2014).
88. J. M. D. Day, K. T. Tait, A. Udry, F. Moynier, Y. Liu, C. R. Neal, Martian magmatism from plume metasomatized mantle. *Nat. Commun.* **9**, 4799 (2018).
89. J. B. Balta, M. Sanborn, H. Y. Mcsween, M. Wadhwa, Magmatic history and parental melt composition of olivine-phyric shergottite LAR 06319: Importance of magmatic degassing and olivine antecrysts in Martian magmatism. *Meteorit. Planet. Sci.* **48**, 1359–1382 (2013).
90. J. H. Jones, Various aspects of the petrogenesis of the Martian shergottite meteorites. *Meteorit. Planet. Sci.* **50**, 674–690 (2015).
91. A. E. Rubin, P. H. Warren, J. P. Greenwood, R. S. Verish, L. A. Leshin, R. L. Hervig, R. N. Clayton, T. K. Mayeda, Los Angeles: The most differentiated basaltic martian meteorite. *Geology* **28**, 1011–1014 (2000).
92. D. A. Kring, J. D. Gleason, T. D. Swindle, K. Nishiizumi, M. W. Caffee, D. H. Hill, A. J. T. Jull, W. V. Boynton, Composition of the first bulk melt sample from a volcanic region of Mars: Queen Alexandra Range 94201. *Meteorit. Planet. Sci.* **38**, 1833–1848 (2003).
93. A. Jambon, V. Sautter, J. A. Barrat, J. Gattacceca, P. Rochette, O. Boudouma, D. Badia, B. Devouard, Northwest Africa 5790: Revisiting nakhlite petrogenesis. *Geochim. Cosmochim. Acta* **190**, 191–212 (2016).
94. M. Humayun, A. Nemchin, B. Zanda, R. H. Hewins, M. Grange, A. Kennedy, J. P. Lorand, C. Göpel, C. Fieni, S. Pont, D. Deldicque, Origin and age of the earliest Martian crust from meteorite NWA 7533. *Nature* **503**, 513–516 (2013).
95. S. Goderis, A. D. Brandon, A. D. B. Mayer, M. Humayun, Ancient impactor components preserved and reworked in Martian regolith breccia Northwest Africa 7034. *Geochim. Cosmochim. Acta* **191**, 203–215 (2016).
96. C. B. Agee, N. V. Wilson, F. M. McCubbin, K. Ziegler, V. J. Polyak, Z. D. Sharp, Y. Asmerom, M. H. Nunn, R. Shaheen, M. H. Thiemens, A. Steele, M. L. Fogel, R. Bowden, M. Glamoclija, Z. Zhang, S. M. Elardo, Unique meteorite from early Amazonian Mars: Water-rich basaltic breccia Northwest Africa 7034. *Science* **339**, 780–785 (2013).
97. A. D. Brandon, I. S. Puchtel, R. J. Walker, J. M. D. Day, A. J. Irving, L. A. Taylor, Evolution of the martian mantle inferred from the ^{187}Re–^{187}Os isotope and highly siderophile element abundance systematics of shergottite meteorites. *Geochim. Cosmochim. Acta* **76**, 206–235 (2012).
98. K. T. Tait, J. M. D. Day, Chondritic late accretion to Mars and the nature of shergottite reservoirs. *Earth Planet. Sci. Lett.* **494**, 99–108 (2018).
99. M. Paquet, J. M. D. Day, A. Udry, R. Hattingh, B. Kumler, R. R. Rahib, K. T. Tait, C. R. Neal, Highly siderophile elements in shergottite sulfides and the sulfur content of the martian mantle. *Geochim. Cosmochim. Acta* **293**, 379–398 (2021).
100. R. J. Baumgartner, M. L. Fiorentini, J. P. Lorand, D. Baratoux, F. Zaccarini, L. Ferrière, M. K. Prašek, K. Sener, The role of sulfides in the fractionation of highly siderophile and chalcophile elements during the formation of martian shergottite meteorites. *Geochim. Cosmochim. Acta* **210**, 1–24 (2017).
101. I. Leya, J. Hirtz, J.-C. David, Galactic cosmic rays, cosmic-rays variations and cosmogenic nuclides in meteorites. *Astrophys. J.* **910**, 136 (2021).
102. S. Agostinelli, J. Allison, K. Amako, J. Apostolakis, H. Araujo, P. Arce, M. Asai, D. Axen, S. Banerjee, G. Barrand, F. Behner, L. Bellagamba, J. Boudreau, L. Broglia, A. Brunengo, H. Burkhardt, S. Chauvie, J. Chuma, R. Chytracek, G. Cooperman, G. Cosmo, P. Degtyarenko, A. Dell'Acqua, G. Depaola, D. Dietrich, R. Enami, A. Feliciello, C. Ferguson, H. Fesefeldt, G. Folger, F. Foppiano, A. Forti, S. Garelli, S. Giani, R. Giannitrapani, D. Gibin, J. J. Gómez Cadenas, I. González, G. Gracia Abril, G. Greeniaus, W. Greiner, V. Grichine, A. Grossheim, S. Guatelli, P. Gumplinger, R. Hamatsu, K. Hashimoto, H. Hasui, A. Heikkinen, A. Howard, V. Ivanchenko, A. Johnson, F. W. Jones, J. Kallenbach, N. Kanaya, M. Kawabata, Y. Kawabata, M. Kawaguti, S. Kelner, P. Kent, A. Kimura, T. Kodama, R. Kokoulin, M. Kossov, H. Kurashige, E. Lamanna, T. Lampén, V. Lara, V. Lefebure, F. Lei, M. Liendl, W. Lockman, F. Longo, S. Magni, M. Maire, E. Medernach, K. Minamimoto, P. Mora de Freitas, Y. Morita, K. Murakami, M. Nagamatu, R. Nartallo, P. Nieminen, T. Nishimura, K. Ohtsubo, M. Okamura, S. O'Neale, Y. Oohata, K. Paech, J. Perl, A. Pfeiffer, M. G. Pia, F. Ranjard, A. Rybin, S. Sadilov, E. di Salvo, G. Santin, T. Sasaki, N. Savvas, Y. Sawada, S. Scherer, S. Sei, V. Sirotenko, D. Smith, N. Starkov, H. Stoecker, J. Sulkimo, M. Takahata, S. Tanaka, E. Tcherniaev, E. Safai Tehrani, M. Tropeano, P. Truscott, H. Uno, L. Urban, P. Urban, M. Verderi, A. Walkden, W. Wander, H. Weber, J. P. Wellisch, T. Wenaus, D. C. Williams, D. Wright, T. Yamada, H. Yoshida, D. Zschiesche, Geant4—A simulation toolkit. *Nucl. Instrum. Methods. Phys. Res. A* **506**, 250–303 (2003).
103. S. Leray, D. Mancusi, P. Kaitaniemi, J. C. David, A. Boudard, B. Braunn, J. Cugnon, Extension of the Liège intra nuclear cascade model to light ion-induced for medical and space applications. *J. Phys. Conf. Ser.* **420**, 012065 (2013).
104. J.-C. David, Spallation reactions: A successful interplay between modeling and applications. *Eur. Phys. J. A* **51**, 68 (2015).
105. C. Villagrasa-Canton, A. Boudard, J.-E. Ducret, B. Fernandez, S. Leray, C. Volant, P. Armbruster, T. Enqvist, F. Hammache, K. Helariutta, B. Jurado, M.-V. Ricciardi, K.-H. Schmidt, K. Sümmerer, F. Vivès, O. Yordanov, L. Audouin, C.-O. Bacri, L. Ferrant, P. Napolitani, F. Rejmund, C. Stéphan, L. Tassan-Got, J. Benlliure, E. Casarejos, M. Fernandez-Ordoñez, J. Pereira, S. Czajkowski, D. Karamanis, M. Pravikoff, J. S. George, R. A. Mewaldt, N. Yanasak, M. Wiedenbeck, J. J. Connell, T. Faestermann, A. Heinz, A. Junghans, Spallation residues in the reaction Fe56^{+}p at 0.3A, 0.5A, 0.75A, 1.0A and 1.5A GeV. *Phys. Rev. C Nucl. Phys.* **75**, 044603 (2007).
106. A. J. Koning, D. Rochman, Modern nuclear data evaluation with the TALYS code system. *Nucl. Data Sheets* **113**, 2841–2934 (2012).
107. R. Wieler, L. Huber, H. Busemann, S. Seiler, I. Leya, C. Maden, J. Masarik, M. M. M. Meier, K. Nagao, R. Trappitsch, A. J. Irving, Noble gases in 18 Martian meteorites and angrite Northwest Africa 7812—Exposure ages, trapped gases, and a re-evaluation of the evidence for solar cosmic ray-produced neon in shergottites and other achondrites. *Meteorit. Planet. Sci.* **51**, 407–428 (2016).
108. G. L. Villanueva, M. J. Mumma, R. E. Novak, H. U. Käufl, P. Hartogh, T. Encrenaz, A. Tokunaga, A. Khayat, M. D. Smith, Strong water isotopic anomalies in the Martian atmosphere: Probing current and ancient reservoirs. *Science* **348**, 218–221 (2015).
109. G. F. Herzog, M. W. Caffee, Cosmic-ray exposure ages of meteorites, in *Treatise on Geochemistry: Meteorites and Cosmochemical Processes* (Elsevier, 2014), vol. 1, pp. 419–454.
110. H. C. Aoudjehane, G. Avice, J.-A. Barrat, O. Boudouma, G. Chen, M. J. M. Duke, I. A. Franchi, J. Gattacceca, M. M. Grady, R. C. Greenwood, C. D. K. Herd, R. Hewins, A. Jambon, B. Marty, P. Rochette, C. L. Smith, V. Sautter, A. Verchovsky, P. Weber, B. Zanda, Tissint martian meteorite: A fresh look at the interior, surface, and atmosphere of Mars. *Science* **338**, 785–788 (2012).

Acknowledgments: We appreciate the two anonymous reviewers for constructive comments and B. Schoene for editorial handling of the manuscript. We thank R. Brasser for discussion on various aspects of this paper. **Funding:** Financial support for this project was provided by grants from the Carlsberg Foundation (CF18_1105) and the European Research Council (ERC Advanced Grant Agreement 833275—DEEPTIME to M.B. and ERC Consolidator Grant Agreement 101001282—METAL to F.M.) and grants from the Carlsberg Foundation (CF20_0209) and the Villum Fonden (00025333) to M.S. Additional support was provided from the UnivEarthS Labex program (ANR-10-LABX-0023 and ANR-11-IDEX-0005-02). K.Z. was supported by fellowships from China Scholarship Council and Alexander von Humboldt Foundation. **Author contributions:** The research was designed by K.Z., M.S., F.M., and M.B. Sample preparation, chemical purification, and mass spectrometry were performed by K.Z., M.S., N.S.S., K.K.L., E.A., and C.R. Impact models were produced by L.P. M.S. and M.B. developed the fractional crystallization and assimilation models. I.L. performed the spallogenic production rate calculations. All authors participated in the interpretation of the data. The manuscript was written by K.Z. and M.B. with input from all authors. **Competing interests:** The authors declare that they have no competing interests. **Data and materials availability:** All data needed to evaluate the conclusions in the paper are present in the paper and/or the Supplementary Materials.

Submitted 6 March 2022
Accepted 27 September 2022
Published 16 November 2022
10.1126/sciadv.abp8415

Science Advances

Late delivery of exotic chromium to the crust of Mars by water-rich carbonaceous asteroids

Ke ZhuMartin SchillerLu PanNikitha Susan SajiKirsten K. LarsenElsa AmsellemCourtney RundhaugPaolo SossiIngo LeyaFrederic MoynierMartin Bizzarro

Sci. Adv., 8 (46), eabp8415. • DOI: 10.1126/sciadv.abp8415

Science Advances (ISSN) is published by the American Association for the Advancement of Science. 1200 New York Avenue NW, Washington, DC 20005. The title *Science Advances* is a registered trademark of AAAS.